The Shear Flow Processing of Controlled DNA Tethering and Stretching for Organic Molecular Electronics

Guihua Yu,[†] Amit Kushwaha,[‡] Jungkyu K. Lee,[§] Eric S. G. Shaqfeh,[†,‡,*] and Zhenan Bao[†,*]

[†]Department of Chemical Engineering, Stanford University, Stanford, California 94305, United States, [‡]Department of Mechanical Engineering, Stanford University, Stanford, California 94305, United States, and [§]Department of Chemistry, Stanford University, Stanford, California 94305, United States

ABSTRACT DNA has been recently explored as a powerful tool for developing molecular scaffolds for making reproducible and reliable metal contacts to single organic semiconducting molecules. A critical step in the process of exploiting DNA—organic molecule—DNA (DOD) array structures is the controlled tethering and stretching of DNA molecules. Here we report the development of reproducible surface chemistry for tethering DNA molecules at tunable density and demonstrate shear flow processing as a rationally controlled approach for stretching/aligning DNA molecules of various lengths. Through enzymatic cleavage of λ-phage DNA to yield a series of DNA chains of various lengths from 17.3 μm down to 4.2 μm, we have investigated the flow/extension behavior of these tethered DNA molecules under different flow strengths in the flow-gradient plane. We compared Brownian dynamic simulations for the flow dynamics of tethered λ-DNA in shear, and found our flow-gradient plane experimental results matched well with our bead—spring simulations. The shear flow processing demonstrated in our studies represents a controllable approach for tethering and stretching DNA molecules of various lengths. Together with further metallization of DNA chains within DOD structures, this bottom-up approach can potentially enable efficient and reliable fabrication of large-scale nanoelectronic devices based on single organic molecules, therefore opening opportunities in both fundamental understanding of charge transport at the single molecular level and many exciting applications for ever-shrinking molecular circuits.

KEYWORDS: DNA stretching · shear flow · tethering · extension · molecular electronics

The field of molecular electronics which explores molecular building blocks for the fabrication of ever-shrinking electronic elements is an exciting interdisciplinary research area that spans physics, chemistry, and materials science.[1−6] Much of the excitement of this area has arisen from the huge prospect of size reduction in electronics offered by the molecular-level control of their properties.[4,7−9] However, one of the biggest obstacles for molecular electronics to be practically exploited, especially single molecule electronics, which involves the smallest stable structures for the ultimate goal of the miniaturization, is the lack of techniques to make reliable and reproducible electrical contacts to single organic molecules of interest. To this end, a number of techniques for probing electrical transport through single organic molecules or through a monolayer of organic molecules have been reported, including mechanical break junctions,[10,11] electromigration-induced gaps,[12−14] nanoscale patterning,[15] scanning probe microscopy (SPM),[8,16,17] metallic cross-wire structures,[18] and vertical metal—monolayer—metal structures.[19−21] Although these methods have produced exciting new results on electrical transport at the molecular level, there still remain critical challenges in creating reproducible and well-defined contacts between metal electrodes and individual single molecules, thus further extending their large-scale applications in nanoelectronics and nanoscale opto-electronics.[22,23]

One promising strategy we envisioned to address this challenge is to exploit DNA, one of the most versatile and powerful molecules available for molecular fabrication and self-assembly, as a molecular template for metal electrodes. DNA molecules are ideal for this purpose because not only can they be chemically linked to a variety of single organic molecules[24−26] but they can also be used as a template for metallic nanostructures,[27,28] thus forming in-place electrical contacts to the center organic single molecule. Specifically, our proposed strategy starts with the synthesis of hybrid DNA—organic molecule—DNA (DOD) structures, followed by subsequent stretching/alignment and double tethering of the DOD assemblies between two microscopic metal electrodes. Further metallization of the DNA segments completes the fabrication of metal electrode—organic molecule—metal electrode (M—O—M) structures, thus realizing the conducting contacts to organic single molecules. Our approach that utilizes DNA as a templated

*Address correspondence to esgs@stanford.edu, zbao@stanford.edu.

Received for review October 6, 2010 and accepted November 17, 2010.

Published online December 2, 2010. 10.1021/nn102669b

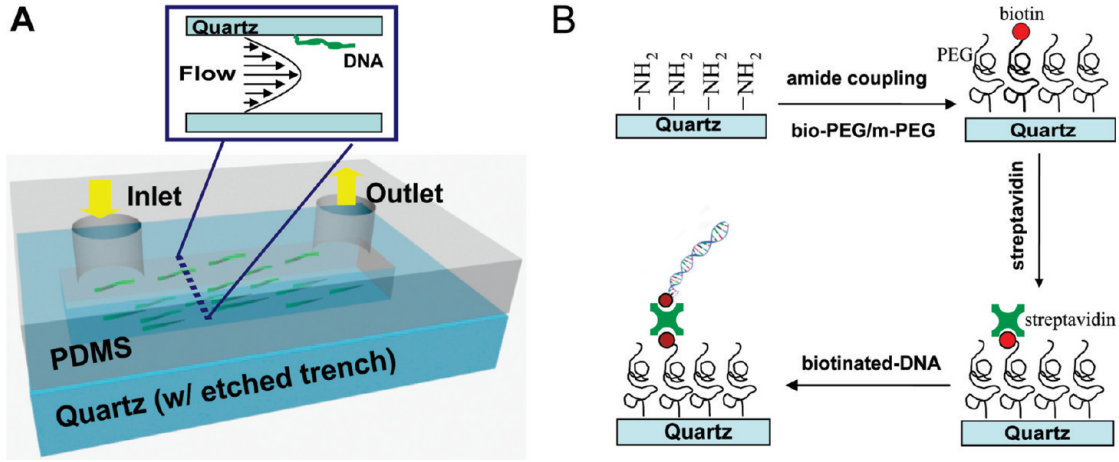

Figure 1. (A) Schematic illustration of experimental flow cell setup. A quartz coverslip with laser etched trench (5 mm ×1 mm ×0.1 mm) as microfluidic channel is placed in close contact with PDMS backing with two holes serving respectively as inlet and outlet. Pressure-driven Poiseuille flow through the rectangular microchannel leads to simple shear very near each wall. Inset, top view image of microfluidic channel showing a DNA molecule (green) tethered to sidewall in the flow-gradient plane. (B) Schematic illustration of experimental steps for controlled tethering DNA molecules onto quartz substrate surfaces. The biotin−streptavidin linkage is exploited as tethering chemistry in our experiments, and through adjusting the ratio of methoxyl-PEG and biotin-PEG to limit the binding sites available for biotinylated DNA molecules, controlled DNA tether density can be achieved.

bridge to connect single organic molecules and microscopic electrodes is a bottom-up approach to integration at the nanoscale. It represents an important step toward the building of increasingly complex molecular circuits.

Recent progress has been made in the synthesis of these DOD hybrid polymer structures each of which has a typical total length of several micrometers (1−4 μm);[26,29] however, limited progress has been achieved in developing an approach for the controlled tethering and precise stretching of DNA chains, especially short DNA molecules within DOD assemblies. Here, we develop a reproducible tethering process based on biotin−streptavidin linkage chemistry for tethering DNA molecules at tunable density to surfaces, and more importantly, we demonstrate a shear flow processing as a powerful means for the precise control of stretching and orienting tethered DNA chains of various lengths from ~17 μm down to ~4 μm. These results on the extension behavior of tethered DNA chains in shear flow provide a guide for the rational control of stretching and aligning DOD structures given that the bending rigidity of the DNA backbone at this length scale plays a key role in the shear flow processing.

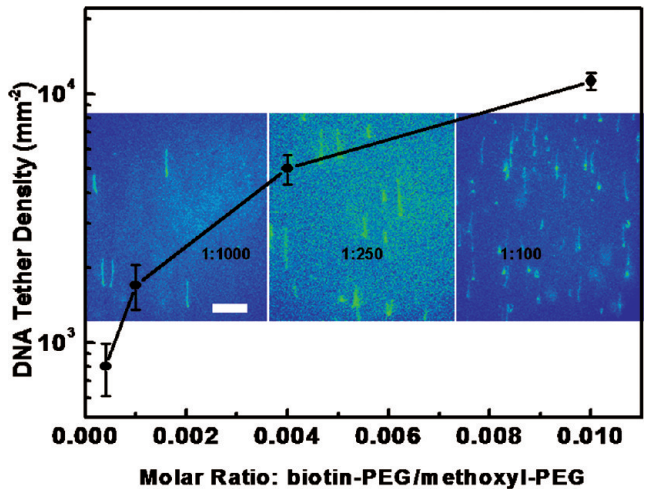

Figure 2. DNA tethering density versus molar ratio of biotin-PEG/methoxyl-PEG plot showing control of tethered DNA density by adjusting the ratio of biotin-PEG and methoxyl-PEG. Insets, optical fluorescence images of various density DNA molecules tethered to quartz surfaces with respect to molar ratio of biotin-PEG/methoxyl-PEG: 1:1000, 1:250, and 1:100 respectively. Scale bar of 10 μm is the same for all three images. The direction of flow is from top to bottom.

Single DNA molecules can be stretched and manipulated by different flow fields,[30,31] and their dynamics in flow have been extensively studied.[32] The stretching of tethered DNA chains subject to shear flow has been previously studied via simulation by Schroeder et al. and Zhang et al.,[33,34] and experimentally in the flow-vorticity plane by Ladoux and Doyle;[35,36] however, it is still underexplored for chain dynamics of different-length DNA molecules in the flow-gradient plane. In this article, we investigated for the first time the flow extension behavior of a series of tethered DNA molecules of different lengths (17.3, 7.8, and 4.2 μm) under various flow strengths in the flow-gradient plane. When compared with our Brownian dynamic simulations for the shear dynamics of tethered λ-DNA chains, our flow-gradient plane results are found to be in good agreement with our bead−spring (BS) simulations.

Imaging tethered DNA molecules in the flow-gradient plane under the influence of shear flow was accomplished by tethering one end of a fluorescently stained DNA molecule to the edge of a microfluidic channel with a rectangular cross section, as shown schematically in Figure 1A. The fluorescently labeled DNA molecules were then visualized using an epi-fluorescence microscope (Nikon Eclipse TE3000), and

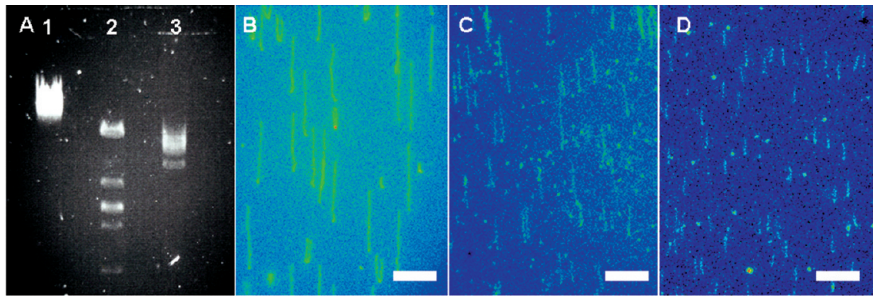

Figure 3. Tethered DNA with various lengths through enzymatic cleavage of biotinylated λ-DNA molecules. (A) Gel electrophoresis image showing the cleavage results by different restriction enzymes: (lane 1) biotinylated λ-DNA sample as control; (lane 2) *Eco*RI enzyme-cleaved DNA sample yielding five different bands (the top one corresponds to 21.2 kbp), (lane 3) *Pvu*I enzyme-cleaved DNA sample yielding three different bands with the middle one corresponding to a mixture of 11.9 kbp and 12.7 kbp segments. (B) Optical fluorescence image of λ-DNA molecules tethered to quartz substrates with uniform length of ~14 μm, which is 80% extension of full λ-DNA length. (C, D) Optical fluorescence images showing 21.2 kbp DNA molecules cleaved by *Eco*RI and 11.9 kbp DNA molecules cleaved by *Pvu*I, both of which were successfully tethered to the substrate surface with relatively uniform lengths of ~6.4 μm and ~3.5 μm, which is about 80% extension of their respective full length. The scale bar of 10 μm is the same for all three images B–D. The direction of flow is from top to bottom.

the images/movies were recorded through image capture software (Compix SimplePCI 6.0) and further imported to Matlab for image analysis.[37]

To realize a reproducible tethering process, we exploited the well-established biotin-streptavidin linkage chemistry to tether DNA molecules to surfaces.[38] The basic steps in our approach as illustrated in Figure 1B consist of functionalizing the surface with amine-terminated silanes, reacting the amines with *N*-hydroxysuccinimide (NHS)-functionalized polyethylene glycol (PEG) chains that are terminated with biotin, and using an avidin derivative to create a link to a biotin-terminated DNA molecule (see Supporting Information). Significantly, we are able to tune the tethering density of DNA molecules on substrate surfaces over at least an order of magnitude by adjusting the ratio of biotin-terminated PEG and methoxyl-terminated PEG. The DNA tether density vs PEG molar ratio plot in Figure 2 shows a clear increase in DNA tethering density on bottom surfaces of quartz flow cells as the molar ratio of biotin-PEG and methoxyl-PEG increases from 1:2500 to 1:100. In our experiments of flowing the solution of biotinylated DNA for an optimal 5 min (fixed exposure time of the biotinylated DNA to the streptavidin-activated surface), we found that the DNA tethering density can be varied over more than an order of magnitude from $8.0 \pm 1.9 \times 10^2$ to $11.3 \pm 0.9 \times 10^3$ mm^{-2} as the ratio of biotin-PEG vs methoxyl-PEG increases from 0.0004 (1:2500) to 0.01 (1:100). Representative optical fluorescence images of λ-DNA molecules with different tethering densities on derivatized surfaces (insets, Figure 2) show that the tethered DNA are well separated with spacing from several tens of micrometer to a few micrometers and, moreover, have good orientational alignment following the direction of shear flow.

The demonstrated capability to control the DNA tethering density and the spacing between tethered DNA molecules allows the pursuit of optimized imaging conditions to study the shear flow behavior of single DNA chains tethered to the sidewall of microchannels since the fluorescently stained DNA molecules need be reasonably separated for visualization analysis. We found the best ratio of biotin-PEG/methoxyl-PEG is 1:250 in our studies in order to obtain a reasonable surface density of tethered DNA molecules on the sidewall while avoiding any crosstalk between neighboring DNA chains. Besides controlling the tethering density, the PEGylation reaction step serves additional purposes for our experiments: PEG molecules act as spacers for facile surface binding, and meanwhile methoxyl-PEG can passivate the surface to prevent nonspecific adsorption of avidin derivatives or DNA molecules.

By selectively cutting λ-DNA molecules using a variety of restriction enzymes to yield segments of various lengths, we were able to systematically investigate chain-length dependence of flow dynamic behavior in shear, offering direct insight to precisely control the stretching and alignment of DNA chains of various lengths. To create a series of tethered DNA chains of different lengths, we have exploited a unique strategy that separates the enzymatic cleavage process of biotinylated λ-DNA and the tethering process during which only the first enzyme-cut DNA segments bearing a biotin end group can selectively bind to the derivatized surface on substrates. For example, we chose two different restriction enzymes to cleave λ-DNA, namely *Eco*RI and *Pvu*I, in order to study the flow extension behavior of a series of DNA chains of lengths $L =$ 17.3 μm (48.5 kbp), 7.8 μm (21.2 kbp), and 4.2 μm (11.9 kbp), respectively.

Agarose gel electrophoresis was used to characterize the digested fragments of biotinylated λ-DNA samples. Figure 3A shows the gel electrophoresis image of three different samples: biotinylated λ-DNA as control (lane 1), *Eco*RI-digested fragments (lane 2), and *Pvu*I-digested fragments (lane 3). While lane 1 from the control sample of λ-DNA exhibits only one band, we observed five bands, as expected, on the gel lane 2 which

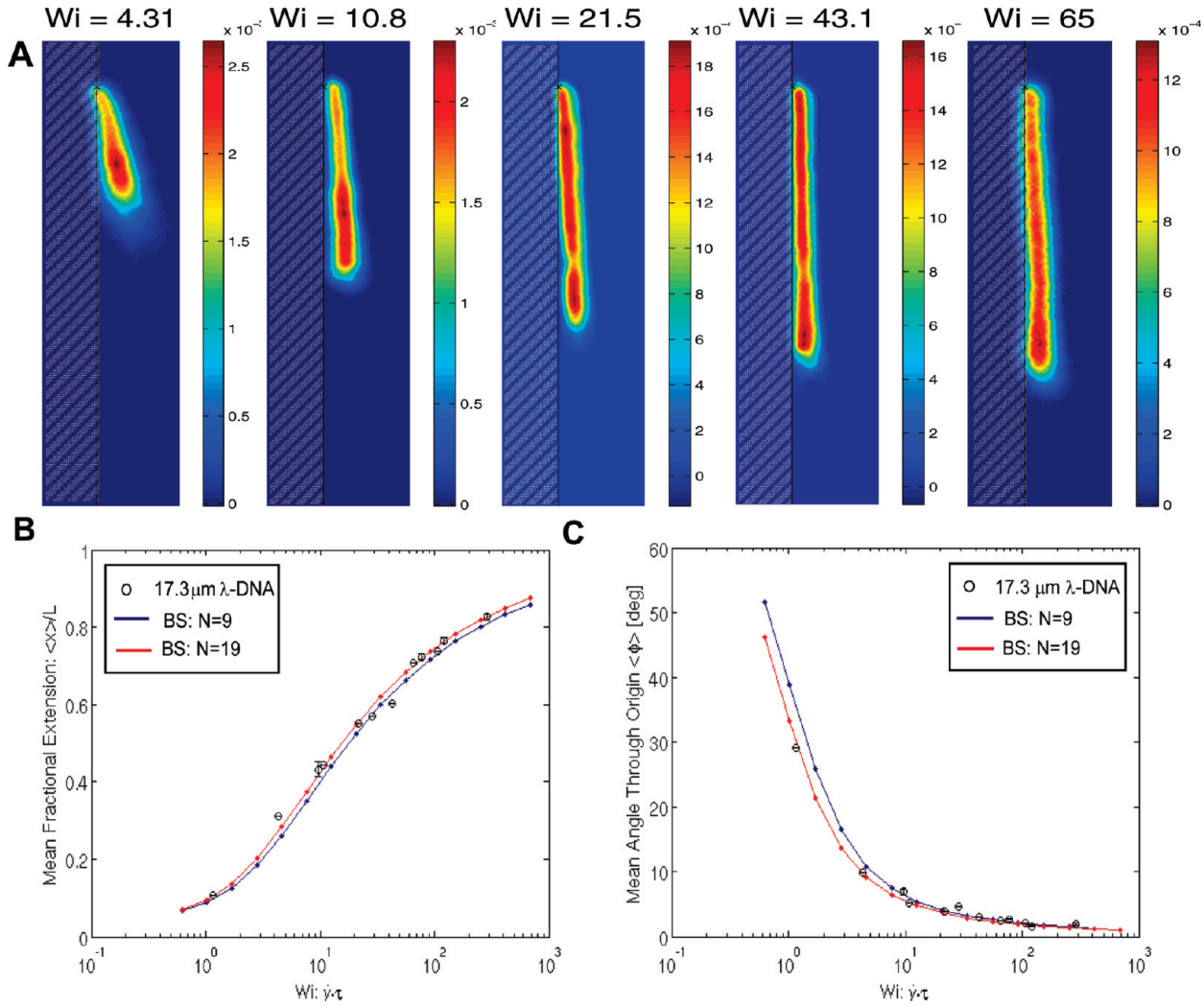

Figure 4. (A) Ensemble images showing average configuration of λ-DNA molecules at various flow strengths Wi. Ensemble images are created by extracting a region of interest for each frame captured and summing all regions for one DNA molecule. The height of each experimental image shown here is 21 μm (corresponding to ~120% of full extension of tethered λ-DNA). (B) Mean fractional extension vs flow strength. Experimental results for 17.3 μm λ-DNA agree well with BS simulation results. (C) Mean orientation angle through origin vs flow strength. Experimental results are in good agreement with our BS simulations, with the orientation angle showing a sharp decay up to *Wi* ≈ 10 due to an increase in extension and a decrease in distance from wall.

are attributed to five different locations of sites cleaved by *Eco*RI with the top band corresponding to a 21.2 kbp segment, and three bands on the gel lane 3 confirming the successful cleavage by *Pvu*I (the top two bands are very close to each other due to the difficulty of distinguishing 11.9, 12.7, and 14.3 kbp segments).[39] More importantly, representative optical images of DNA tethering results from three different solutions (Figure 3B−D) demonstrate well-aligned and controlled density DNA chains of relatively uniform length successfully tethered to quartz surfaces. These results further confirm the feasibility of our approach of separating the enzyme digest process and the biotin−DNA−streptavidin tethering process, which offers a higher yield of DNA digest and better uniformity of the lengths of tethered DNA compared to the results from in situ enzyme cleavage during flow.

To systematically investigate the behavior of DNA molecules in shear (such as flow extension, chain distance from the wall, and orientation angle) to determine the dependence on flow strength, we use the dimensionless Weissenberg number, $Wi = \tau\dot{\gamma}$, where $\dot{\gamma}$ is the shear rate and τ is the longest DNA relaxation time, to characterize the strength of shear flow. At a small *Wi*, the flow is weak, and the time scale for the dynamics of the polymer is governed by the relaxation time, whereas at a high *Wi* the flow is strong and the time scale for the dynamics is governed by $1/\dot{\gamma}$. To determine the relaxation time τ for different DNA chain lengths, we performed a series of standard extension−relaxation experiments which involved stretching the chains at a high shear rate to >80% extension $\langle x\rangle/L$, stopping the flow and measuring the free relaxation of the chains back to their equilibrium coiled configuration.[40] For each length of DNA chains, ensemble averages were taken over 10−15 chains. Given the nonlinear nature of the force−extension behavior where only the last ~30% of extension or last ~9% of

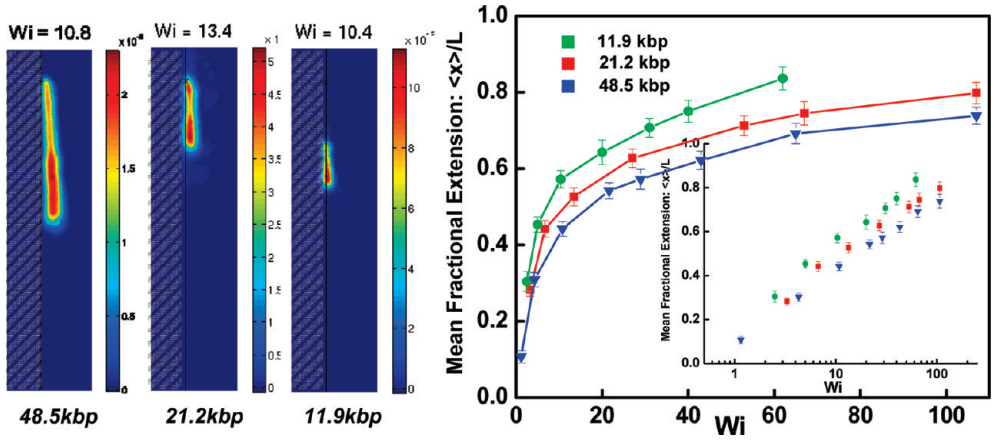

Figure 5. (A) Representative ensemble images of different length DNA molecules at similar flow strength *Wi*. (B) Summary plot showing the average fractional extension as a function of flow strength *Wi* for DNA molecules of various chain lengths. Data points in circle (green), square (red), and triangle (blue), correspond to DNA chain lengths of 11.9 kbp (*Pvu*I cleaved), 21.2 kbp (*Eco*RI cleaved), and 48.5 kbp (full λ-DNA), respectively. Inset, a semilog plot of mean fractional extension versus *Wi*.

square extension is Hookean, the plot of mean square extension $\langle x^2\rangle/L^2$ vs time after flow cessation for an ensemble of chains can be well described and fit to the functional form, $c1\ \exp[-t/\tau] + c2$, where $c1$ and $c2$ are free parameters, and τ is the characteristic relaxation time.[36] We have determined that for this series of 17.3-, 7.8-, and 4.2-μm long tethered DNA molecules in the 261 cP 65% sucrose solution, the longest relaxation times τwere 52.5, 16.5, and 6.1 s, respectively. We further analyzed the relaxation times in terms of their scaling with DNA lengths, and found that $\tau \approx L^{1.55}$, which fits the Zimm model for polymer chains that predicts that the longest relaxation times follow a scaling law as $\tau \approx L^{3\nu}$, with the scaling exponent 3ν depending on solvent quality.[41] Our calculated scaling exponent $3\nu \approx 1.55$ is in good agreement with that measured by others in similar untethered systems ($3\nu \approx 1.65 \pm 0.1$).[32,40]

We have examined in detail the effect of shear flow strength on the tethered DNA chain's conformation in the flow-gradient plane. Figure 4A shows a typical set of two-dimensional (2D) distributions of tethered λ-phage DNA molecules at various flow strengths (varying *Wi*) in the flow-gradient plane. These ensemble images of DNA were obtained by extracting a region of interest where all DNA configurations were exclusively captured for each data frame recorded (typical time step between frames: 1−3 s; exposure time: 0.15−0.25 s; data frames usually taken after 5 min when flow rate was initiated or changed in order to reach steady state) and summing all regions for one DNA molecule. We can clearly see from ensemble images that, as the flow strength *Wi* increases (e.g., from 4.3 to 65), the average extension accordingly increases monotonically from ~30% to ~65%. Moreover, we find our ensemble-averaged images from experiments are in good qualitative agreement with those based on the BS simulations of free-draining wormlike chains we developed recently.[37] We also observed that at the low flow rate (e.g. $Wi = 4.3$, or 10.8), the experimental ensemble images showed an intense peak close to the middle of the distribution with lower intensity near the end, which is due to the presence of cyclic dynamics (Figure S1, Supporting Information [SI]), an interesting phenomenon occurring for tethered DNA chains at moderate flow strength.[35] Furthermore, we summarized several key parameters in the system such as mean fractional extension $\langle x\rangle/L$ and mean orientation angle through origin ϕ (Figure 4B,C). We can see that our experimental results are consistent with the BS simulations.

More importantly, we have systematically investigated the shear flow extension of DNA chains of all three different lengths (Figure 5, Figure S2 [SI]). Representative ensemble images in Figure 5A show respective average configuration of three different-length DNA molecules at similar flow strength *Wi*. Note that a much larger flow rate is required to match the flow strength *Wi* for shorter DNA molecules given the difference in the longest relaxation times we mentioned above for various chain lengths. We have further performed quantitative analyses on the mean fractional extension of these tethered DNA chains in the flow direction. The curves of the average fractional extension $\langle x\rangle/L$ versus flow strength *Wi* for three different chain length DNA are plotted and summarized in Figure 5B. Experimental averages at each *Wi* were taken over ensemble averages of 10−15 DNA molecules with time averages of 5−10 min for each molecule. Several key features are shown in the summary plot in Figure 5B. First, all the chains showed a progressive and rapid increase in average fractional extension up to $Wi \approx 20$. At a larger *Wi* the chains continued to stretch with mean fractional extension slowly approaching unity (full extension). This is distinct from the extension of a DNA polymer in free shear flow which is known to plateau around 50% of its contour length because of the tumbling dynamics.[33] Second, it is apparent that the data points for three chain lengths formed three separate

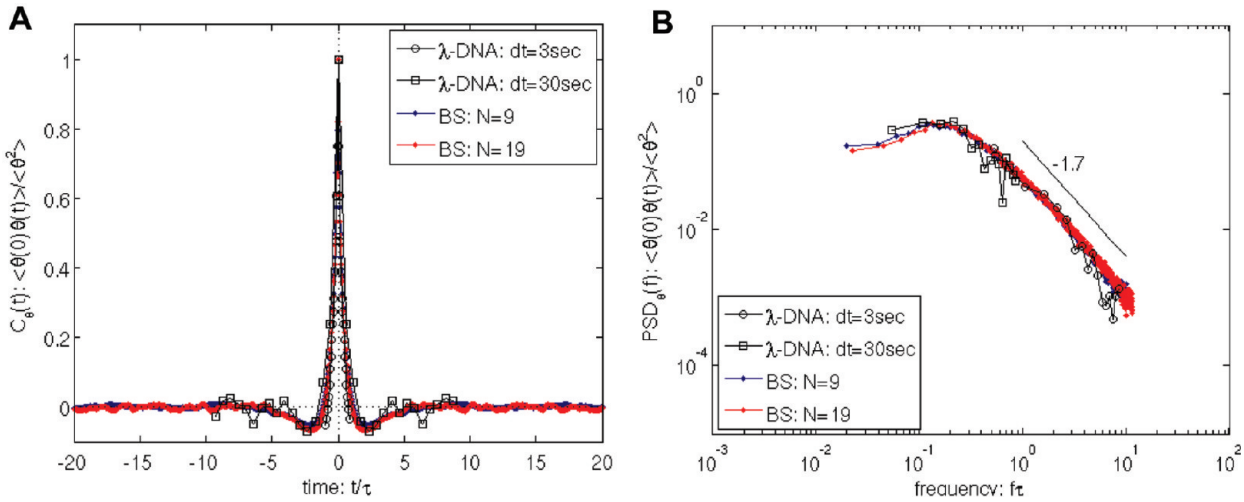

Figure 6. (A) Autocorrelation of orientation angle through the center of mass at *Wi* ≈ 4.3. Experimental results for 17.3 μm λ-DNA agree very well with our BS simulation results. The prominent minimum in the autocorrelation is well resolved experimentally and with simulations. (B) The corresponding PSD of orientation angle through the center of mass at *Wi* ≈ 4.3 decays with a power of −1.7. Experimental results clearly agree with our BS simulations. Note that a clearly resolved peak is present in both experimental and simulation curves at $f\tau \approx 0.18$. This peak represents the most common frequency of the cyclic motion and proves that cyclic motion is quasi-periodic in the system.

traces with the curve for shortest DNA chain (~4.2 μm) clearly deviating from the other two. A smaller *Wi*, accordingly the weaker flow strength, is needed to achieve the same fractional extension and stretching for shorter length DNA molecules. For example, to achieve >80% mean flow extension, the required experimental flow strength was found to be *Wi* ≈ 55, 110, 200 for *L* = 11.9, 21.2, and 48.5 kbp, respectively. This trend could be associated with the finite extensibility of DNA chain playing a key role due to the extension in the flow direction. In addition, we characterized the mean distance from wall and mean orientation angle through origin for all three lengths of tethered DNA molecules, as summarized in Figure S3 [SI]. Our experimental results represent a first and crucial step toward understanding and optimizing the shear flow processing for controlled DNA stretching and anchoring onto surfaces, opening up opportunities in a variety of applications of tethered DNA arrays.

In addition to the average flow extension properties for tethered DNA molecules in shear flow at varying *Wi*, we have quantified the cyclic dynamics in the system that results from the competition between flow-induced drag on DNA chains and Brownian diffusion.[35] For example, we have calculated various correlation functions of the measured experimental variables including extension *x*, chain distance from the wall δ, orientation angle through the center of mass (COM) θ and angle through the tethering origin φ. Cross-correlation functions with the form $C_{XY}(T) = (E[(X(t + T) - \bar{X})(Y(t) - \bar{Y})])/(\sigma_X\sigma_Y)$, where $\bar{X}\bar{Y}$ is the average value of variable *X* and *Y* and $\sigma_X\sigma_Y$ is the standard deviation, and their power spectral density functions with the form $PSD(\nu) = \|\int_{-\infty}^{+\infty} C_{XY}(T) \exp(-2i\pi\nu T)\, dT\|$ can be used to examine the presence of quasi-periodicity in cyclic dynamics.[37,42] Our experimental correlation functions were calculated by taking a time average and a chain ensemble average over individual trajectories taken in different frames.

The autocorrelation function $C_x(T) = (E[(x(t + T) - \bar{x})(x(t) - \bar{x})])/(\sigma_x^2)$ for orientation angle through COM θ and its corresponding power spectral density are shown in Figure 6. We can see that our experimental results agree well with the BS simulations results for both autocorrelation and PSD.[37] More significantly, the prominent minimum in the autocorrelation and the corresponding peak in the PSD are well resolved both experimentally and by simulations. Indeed, the minimum in the autocorrelation represents a strong negative correlation between increases in orientation angle and a subsequent decrease. The negative correlation can be attributed to the fact that the orientation angle captures the connection between increases in height and a delayed increase in extension therefore showing a clear minimum in contrast to subtle or no periodicity seen in the autocorrelation functions of height or extension. It is also apparent that as shown in Figure 6, the characteristic frequency of cyclic motion at *Wi* ≈ 4.3 is ~0.18, which matches very well with that calculated from bead spring simulations of 0.17 ± 0.03 at *Wi* = 4.6.

In conclusion, we have developed a simple and reproducible method based on shear flow processing for anchoring and stretching DNA molecules of various lengths with tunable density and controlled chain extension. We have also presented the flow-gradient plane experiments to examine the extension behavior of a series of tethered DNA chains with different lengths ranging from 17.3 μm down to 4.2 μm under shear flow for the first time using single-molecule fluores-

cence microscopy. Experiments in the flow gradient plane have revealed the details of cyclic dynamics and confirmed the quasi-periodicity in the system through the analysis of correlation functions and power spectral density functions of orientation angles.

The shear flow processing demonstrated in this study represents a powerful and controllable approach for the precise control over the stretching and alignment of varying length DNA chains and provides a general platform for the flow dynamics study of single DNA molecules. This work is an important step toward building DNA-templated single-molecule electronic devices that can produce precise and reproducible electrical contacts to organic semiconducting molecules. Currently we are working on a repeatable and controllable double tethering process with the aid of the results presented here, and meanwhile developing in situ DNA metallization for ultimately enabling efficient fabrication of large-scale nanoelectronic devices based on single organic molecules.

METHODS

Flow Cell and Imaging Solutions. The flow cell we used is a quartz slide (dimension: 25 mm L × 25 mm W × 0.25 mm H, Technical Glass Products, Inc.) which has a 5 mm ×1 mm ×0.1 mm laser etched rectangular channel. The pressure-driven Poiseuille flow through this rectangular microchannel, which is in close contact with a PDMS backing with two holes serving as the inlet and outlet, results in simple shear very near each wall. To achieve the optimal imaging resolution of tethered DNA molecules, we used 65% (m/m) sucrose buffer solution that has a matching refractive index of 1.4585 at 588 nm to the index of fused quartz.[37] The viscosity of this sucrose buffer is 261 ± 5 cP therefore further enhancing the shear extension of DNA molecules.

DNA Digestion and Tethering. Typically for DNA enzyme digests, we prepared a small scale of 20 μL volume containing 14 μL of distilled water (GIBCO), 2 μL of 10× enzyme buffer (New England Biolabs), 3 μL of biotinylated l-DNA, 1 μL of restriction enzyme (New England Biolabs), and incubated the digest mixture at 37 °C for 30 min. Subsequently, DNA digest solution (5 μL) together with Sytox green (1 μL) were added into a TE buffer (100 μL), and the mixture was subsequently introduced into the microchannel allowing enzyme-cleaved biotinylated DNA segments to bind to streptavidin modified surfaces.

Acknowledgment. We thank Dr. Christopher A. Lueth for his valuable input and help in some experimental setup. E.S.G.S and Z.B. acknowledge the funding support from the Nanoscale Interdisciplinary Research Team, a National Science Foundation funded organization (NSF-NIRT) under Grant DMR-0507296.

Supporting Information Available: Experimental details for DNA tethering procedure, the trajectories showing cyclic dynamics of tethered λ-DNA in shear, additional ensemble images of three different-length DNA molecules at various flow strengths mean distance from wall and mean orientation angle vs flow strength for three different lengths of DNA. This material is available free of charge via the Internet at http://pubs.acs.org.

REFERENCES AND NOTES

1. Tour, J. M., *Molecular Electronics: Commercial Insights, Chemistry, Devices, Architectures and Programming*; World Scientific: River Edge, NJ, 2003.
2. Guo, X.; Small, J. P.; Klare, J. E.; Wang, Y.; Purewal, M. S.; Tam, I. W.; Hong, B. H.; Caldwell, R.; Huang, L.; O'Brien, S.; et al. Covalently Bridging Gaps in Single-Walled Carbon Nanotubes with Conducting Molecules. *Science* **2006**, *311*, 356–359.
3. Porath, D.; Bezryadin, A.; de Vries, S.; Dekker, C. Direct Measurement of Electrical Transport through DNA Molecules. *Nature* **2000**, *403*, 635–638.
4. Heath, J. R.; Ratner, M. A. Molecular Electronics. *Phys. Today* **2003**, *56*, 43–49.
5. Kwok, K. S.; Ellenbogen, J. C. Moletronics: Future Electronics. *Mater. Today* **2002**, *5*, 28–37.
6. Lu, W.; Lieber, C. M. Nanoelectronics from the Bottom Up. *Nat. Mater.* **2007**, *6*, 841–850.
7. Tao, N. J. Electron Transport in Molecular Junctions. *Nature Nanotechnol.* **2006**, *1*, 173–181.
8. Ho Choi, S.; Kim, B.; Frisbie, C. D. Electrical Resistance of Long Conjugated Molecular Wires. *Science* **2008**, *320*, 1482–1486.
9. Moth-Poulsen, K.; Bjornholm, T. Molecular Electronics with Single Molecules in Solid-State Devices. *Nature Nanotechnol.* **2009**, *4*, 551–556.
10. Reed, M. A.; Zhou, C.; Muller, C. J.; Burgin, T. P.; Tour, J. M. Conductance of a Molecular Junction. *Science* **1997**, *278*, 252–254.
11. Smit, R. H. M.; Noat, Y.; Untiedt, C.; Lang, N. D.; van Hemert, M. C.; van Ruitenbeek, J. M. Measurement of the Conductance of a Hydrogen Molecule. *Nature* **2002**, *419*, 906–909.
12. Lee, T.-H.; Hladik, C. R.; Dickson, R. M. Asymmetric Photoconductivity within Nanoscale Break Junctions. *Nano Lett.* **2003**, *3*, 1561–1564.
13. Liang, W.; Shores, M. P.; Bockrath, M.; Long, J. R.; Park, H. Kondo Resonance in a Single-Molecule Transistor. *Nature* **2002**, *417*, 725–729.
14. Park, J.; Pasupathy, A. N.; Goldsmith, J. I.; Chang, C.; Yaish, Y.; Petta, J. R.; Rinkoski, M.; Sethna, J. P.; Abruña, H. D.; McEuen, P. L. Coulomb Blockade and the Kondo Effect in Single-Atom Transistors. *Nature* **2002**, *417*, 722–725.
15. Qin, L.; Park, S.; Huang, L.; Mirkin, C. A. On-Wire Lithography. *Science* **2005**, *309*, 113–115.
16. Cui, X. D.; Primak, A.; Zarate, X.; Tomfohr, J.; Sankey, O. F.; Moore, A. L.; Moore, T. A.; Gust, D.; Harris, G.; Lindsay, S. M. Reproducible Measurement of Single-Molecule Conductivity. *Science* **2001**, *294*, 571–574.
17. Reddy, P.; Jang, S. Y.; Segalman, R. A.; Majumdar, A. Thermoelectricity in Molecular Junctions. *Science* **2007**, *315*, 1568–1571.
18. Blum, A. S.; Kushmerick, J. G.; Long, D. P.; Patterson, C. H.; Yang, J. C.; Henderson, J. C.; Yao, Y.; Tour, J. M.; Shashidhar, R.; Ratna, B. R. Molecularly Inherent Voltage-Controlled Conductance Switching. *Nat. Mater.* **2005**, *4*, 167–172.
19. Zhitenev, N. B.; Meng, H.; Bao, Z. Conductance of Small Molecular Junctions. *Phys. Rev. Lett.* **2002**, *88*, 226801–226804.
20. Akkerman, H. B.; Blom, P. W. M.; de Leeuw, D. M.; de Boer, B. Towards Molecular Electronics with Large-Area Molecular Junctions. *Nature* **2006**, *441*, 69–72.
21. Nitzan, A.; Ratner, M. A. Electron Transport in Molecular Wire Junctions. *Science* **2003**, *300*, 1384–1389.
22. Hipps, K. W. It's All About Contacts. *Science* **2001**, *294*, 536–537.
23. Martin, C. R.; Baker, L. A. Expanding the Molecular Electronics Toolbox. *Science* **2005**, *309*, 67–68.
24. Li, X. Y.; Liu, D. R. DNA-Templated Organic Synthesis. *Angew. Chem., Int. Ed.* **2004**, *43*, 4848–4870.
25. Ustinov, A. V.; Dubnyakova, V. V.; Korshun, V. A. A Convenient 'Click Chemistry' Approach to Perylene Diimide-Oligonucleotide Conjugates. *Tetrahedron* **2008**, *64*, 1467–1473.
26. Lee, J. K.; Jung, Y. H.; Stoltenberg, R. M.; Tok, J. B. H.; Bao, Z.

Synthesis of DNA-Organic Molecule-DNA Triblock Oligomers Using the Amide Coupling Reaction and Their Enzymatic Amplification. *J. Am. Chem. Soc.* **2008**, *130*, 12854–12855.
27. Braun, E.; Eichen, Y.; Sivan, U.; Ben-Yoseph, G. DNA-Templated Assembly and Electrode Attachment of a Conducting Silver Wire. *Nature* **1998**, *391*, 775–778.
28. Keren, K.; Krueger, M.; Gilad, R.; Ben-Yosep, G.; Sivan, U.; Braun, E. Sequence-Specific Molecular Lithography on Single DNA Molecules. *Science* **2002**, *297*, 72–75.
29. Lee, J. K.; Jäckel, F.; Moerner, W. E.; Bao, Z. Micrometer-sized DNA-Single-Fluorophore-DNA Supramolecule: Synthesis and Single-Molecule Characterization. *Small* **2009**, *5*, 2418–2423.
30. Perkins, T.; Smith, D.; Larson, R.; Chu, S. Stretching of a Single Tethered Polymer in a Uniform Flow. *Science* **1995**, *268*, 83–87.
31. Kim, J. H.; Shi, W. X.; Larson, R. G. Methods of Stretching DNA Molecules Using Flow Fields. *Langmuir* **2007**, *23*, 755–764.
32. Shaqfeh, E. S. G. The Dynamics of Single-Molecule DNA in Flow. *J. Non-Newtonian Fluid Mech.* **2005**, *130*, 1–28.
33. Schroeder, C. M.; Teixeira, R. E.; Shaqfeh, E. S. G.; Chu, S. Characteristic Periodic Motion of Polymers in Shear Flow. *Phys. Rev. Lett.* **2005**, *95*, 018301−018304.
34. Jendrejack, R. M.; Schwartz, D. C.; de Pablo, J. J.; Graham, M. D. Shear-Induced Migration in Flowing Polymer Solutions: Simulation of Long-Chain DNA in Microchannels. *J. Chem. Phys.* **2004**, *120*, 2513–2529.
35. Doyle, P. S.; Ladoux, B.; Viovy, J. L. Dynamics of a Tethered Polymer in Shear Flow. *Phys. Rev. Lett.* **2000**, *84*, 4769–4772.
36. Ladoux, B.; Doyle, P. S. Stretching Tethered DNA Chains in Shear Flow. *Europhys. Lett.* **2000**, *52*, 511–517.
37. Lueth, C. A.; Shaqfeh, E. S. G. Experimental and Numerical Studies of Tethered DNA Shear Dynamics in the Flow-Gradient Plane. *Macromolecules* **2009**, *42*, 9170–9182.
38. Savage, M.; Co, P. *Avidin-Biotin Chemistry: A Handbook*; Pierce Chemical Co.: Rockford, IL, 1992.
39. Lambda-DNA cleaved by restriction enzymes: locations of sites. http://www.neb.com/nebecomm/tech_reference/restriction_enzymes/sites/Lambda_sites.pdf.
40. Perkins, T.; Smith, D.; Chu, S. Direct Observation of Tube-Like Motion of a Single Polymer Chain. *Science* **1994**, *264*, 819–822.
41. Zimm, B. H. Dynamics of Polymer Molecules in Dilute Solution: Viscoelasticity Flow Birefringence and Dielectric Loss. *J. Chem. Phys.* **1956**, *24*, 269–278.
42. Chopra, M.; Larson, R. G. Brownian Dynamics Simulations of Isolated Polymer Molecules in Shear Flow Near Adsorbing and Nonadsorbing Surfaces. *J. Rheol.* **2002**, *46*, 831–862.